

Monitoring alkali-aggregate reaction (AAR) induced expansion through the use of fiber Bragg grating sensors

Gustavo Macioski ⁽¹⁾, Leandro F. M. Sanchez ⁽²⁾, Xiaoyi Bao ⁽³⁾, Marcelo H. F. Medeiros ⁽¹⁾

(1) Federal University of Paraná, Post-Graduation Program of Civil Construction Engineering, Curitiba-PR, Brazil, gmacioski@gmail.com, medeiros.ufpr@gmail.com

(2) University of Ottawa, Department of Civil Engineering, Ottawa-ON, Canada, leandro.sanchez@uottawa.ca

(3) University of Ottawa, Department of Physics, Ottawa-ON, Canada, xbao@uottawa.ca

Abstract

Several techniques and procedures were developed over the last decades to perform the condition assessment of concrete infrastructure affected by alkali-aggregate reaction (AAR). Among them, structure health monitoring techniques are deemed as one of the most reliable methods to understand the expansion rate over time and thus the potential of further damage of distressed structures. In this context, Fiber Bragg Grating (FBG) sensors have been gaining increased attention in the market since these optical sensors have small dimensions, low signal loss and high precision for strain measurements. Yet, very few applications of FBG may be found in AAR-affected concrete. This paper aims to evaluate FBG efficiency for appraising expansion in concrete specimens affected by AAR. Concrete cylinders (100 by 200 mm) were fabricated with reactive coarse aggregates and stored at conditions enabling AAR development (38°C and 100% R.H.) as per ASTM C1293. The specimens were monitored over time through the use of distinct approaches such as installed metallic studs and internal and external FBG sensors. Comparisons are made and recommendations on the use of FBG to monitor AAR-induced expansion are performed.

Keywords: durability; optical fiber; damage assessment; structure health monitoring

1. INTRODUCTION

A wide number of distress processes may deteriorate concrete components, yet alkali-aggregate reaction (AAR) is probably one of the most harmful mechanisms affecting concrete infrastructure around the world [26]. AAR is normally divided into two types: alkali-aggregate reaction (ASR) and alkali-carbonate reaction (ACR). ASR is by far the most frequent type of deterioration found worldwide [17]. ASR is defined as a chemical reaction between the alkali hydroxides (Na^+ , K^+ and OH^-) from the concrete pore solution and some unstable siliceous mineral phases from the aggregates used in concrete. ASR provides a product, the so-called ASR gel, that swells under moisture uptake, leading to induced expansion, cracking and mechanical properties reduction [4].

In the last years, standards from different countries were developed, e.g. [1,2,9], in order to establish criteria for assessing, classifying and mitigating ASR in new construction. According to these documents, after an initial petrographic examination where the likely reactive minerals are appraised and described, the best way to assess the behavior of aggregates and/or cement/aggregates combinations in the laboratory is through performance techniques [16]. Performance tests aim to understand the reactivity of aggregates and classify their performance in the laboratory. Normally, performance tests are conducted on mortar bars or concrete prisms, in natural or accelerated conditions [33].

Although the assessment of ASR-induced expansion is relatively well established in the laboratory, the appraisal of ASR expansion rates of affected structures and structural components is much more complicated in the field. AAR usually occurs slowly, which requires the monitoring of the structural components for many years. In bridges or dams, for example, periodic monitoring of expansion and/or displacement of structural members may be performed using steel gauges, electronic sensors or topographic surveys [28]. In this context, optical fiber sensors such as Fiber Bragg Grating (FBG) could be used to evaluate ASR induced expansion. To date, it is not possible to find studies in the literature that assess internal deformations in concrete using FBG. A few researchers evaluated shrinkage [5] and

creep [10,44] over time using optical fiber sensors. Yet, most authors only conduct structural monitoring related to deformations generated by instantaneous loadings [11,12,22–25,32,43]. It is anticipated, thus, that the use of FBG would allow superior precision on ASR expansion measurements, when compared to current steel gauge procedures, enabling temperature corrections automatically.

2. FIBER BRAGG GRATING SENSORS

Optical fiber is a flexible and transparent filament made from extruded glass or plastic and it is used as a conductor of light, images or encoded impulses. It has a diameter of a few micrometers, slightly larger than the human hair [27]. In addition to its application in the telecommunications sector, other technologies started to be developed using this material. In industry, optical fibers are used mainly in telemetry systems (communication to command, measure or track processes). In the medical field, it made it possible to conserve and illuminate the interior of the human body, besides its use in imaging devices, temperature, pressure, pH, and blood flow sensors. In the automaker industry, the applications of fibers range from engine and transmission control to secondary accessories (window control, heating and cooling) [8].

In addition to monitoring, it is possible to apply optical sensors for spot readings during inspections, with the development of new test methodologies for the characterization of materials and equipment based on photonic techniques (field of science dedicated to studying light; its generation, detection, and manipulation of emission, transmission, modulation, signal processing, amplification and sensing) [12,15,27,45].

Thanks to the diffraction phenomenon, it is possible to change the refractive index of the glass in specific sections, periodically, creating an optical filter in the fiber core. This modification is possible due to the photosensitivity of the optical fiber, which allows a permanent change in the refractive index in the fiber core when exposed to ultraviolet (UV) light [40]. After this process, the optical fiber will develop the ability to reflect a specific wavelength depending on the spacing of the grid created in its core. From this light reflection property, the process of acquiring or interrogating a FBG consists of coupling a broadband of light to the fiber, in order to monitor the optical spectrum of the light transmitted or reflected by the FBG, as can be seen in Figure 2.1.

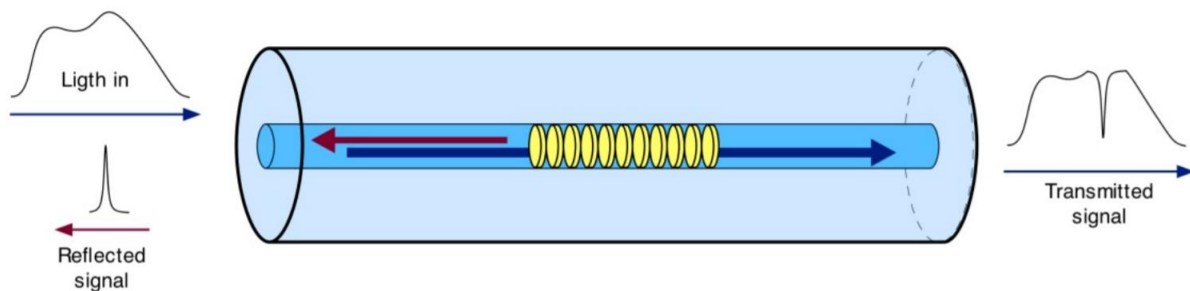


Figure 2.1: Interrogation of FBG based on transmitted and reflected signals [14]

The deformation of the optical fiber causes a change in the period of the microstructure and, consequently, in the Bragg wavelength. This way, the reflected signal can be calibrated according to changes caused in the sensor. When the fiber is pulled or compressed, the FBG sensor can measure its specific deformation [19,30,31].

Optical sensors such as FBG present many advantages when compared to electronic sensors currently available [7,13,20,21,23,24]. FBGs allow the measurement of multiple points using only one fiber and one acquisition channel, and they have superior durability in aggressive environments, due to their non-metallic composition. With small dimensions, optical fiber is a good option for monitoring apparent elements or buildings of historical interest, as it is light, transparent and has a small diameter, becoming almost imperceptible in public places. Because they are electrically passive, optical sensors do not suffer from electromagnetic interference and can be used close to power stations and in places with the incidence of electrical discharges - common in dams and bridges, for example.

Environments with flammable fuels or gases also benefit from the use of optical sensors because they do not need electric current, reducing the risk of explosions. As they do not need to supply electric

current directly to the sensor, they are a solution for structures away from urban centers where there is no electrical supply for the sensors. Another advantage of optical fibers is the low signal loss over long distances, a fact that needs attention when the monitoring method is applied to structures with large spans or with elements far from the signal acquisition equipment. In the case of electronic sensors, it may be necessary to implement signal repeaters and amplifiers so that the data reaches the acquisition system, which is not necessary with the FBG.

However, there must be a production and calibration methodology for each sensor that guarantees a good reading range, high sensitivity, low noise, and adequate acquisition frequency. Therefore, there is still a gap to be filled, since the main applications of optical sensors are still limited to assessing deformations and temperatures. Although these parameters are important in the field of civil construction monitoring, it would be possible to apply optical sensors to measure other properties, internally and externally to the structures.

Hence, it is intended to collaborate with the development of methodologies for the use of optical fiber sensors and to contribute to the application of this technology in the monitoring of deteriorated structures. The use of FBG in civil construction could allow a better investment in the monitoring of assets, thus guaranteeing the integrity of critical infrastructure such as dams, bridges, viaducts, tunnels and even large buildings.

3. MATERIALS AND METHODS

To use FBG to monitor ASR-induced expansion and development, concrete specimens (100 by 200 mm in size) were fabricated using the concrete mix-design as per Table 3.1 and according to ASTM C 1293. A conventional Portland cement (CSA Type GU, ASTM type 1) containing high alkali content (0.88% $\text{Na}_2\text{O}_{\text{eq}}$) was used in the mixture. Reagent grade NaOH was used to raise the total alkali content of the mixtures to 1.25% $\text{Na}_2\text{O}_{\text{eq}}$ by cement mass, for accelerating ASR expansion process.[4].

Table 3.1: Concrete mix design and specific gravity of the materials

Material	Consumption (kg/m ³)	Specific Gravity (g/cm ³)
Cement	426	3,15
Fine aggregate	851	2,64
Coarse aggregate	946	2,71
Water	193	1,00

The reactive greywacke coarse aggregate selected (Springhill Quarry in New Brunswick) presented in previous works [41] expansions around 0.3% after one year. During the molding process, some FBG sensors were inserted in the interior of the concrete samples in different ways. The FBG sensors were glued to some coarse aggregate particles (Figure 3.1a) and then immersed in the concrete during casting. Likewise, FBG sensors were also immersed in the concrete paste. To ensure the protection of the fiberglass against the high pH of the concrete, an epoxy glue coating was used (Figure 3.1b).

After 24 h in their molds (Figure 3.1c), the specimens were demoulded and then placed for another 48 h in a moist curing room. Small holes, 5 mm in diameter by 15 mm long, were then drilled in both ends of each test cylinders and stainless-steel studs were glued in place, with a fast-setting cement slurry, for longitudinal expansion measurements [34–38]. Also, external FBG were glued at the sample surface in vertical and horizontal positions (Figure 3.1d) to measure the sample's expansion over time. The blue colored section of the optical fiber placed in the middle third of the cylinder represents the area where the sensor performs the strain measurement. The number of samples for each FBG positioning can be observed in Table 3.2, where the red arrows represent the FBG sensor direction and its placement (in the concrete surface or internally).

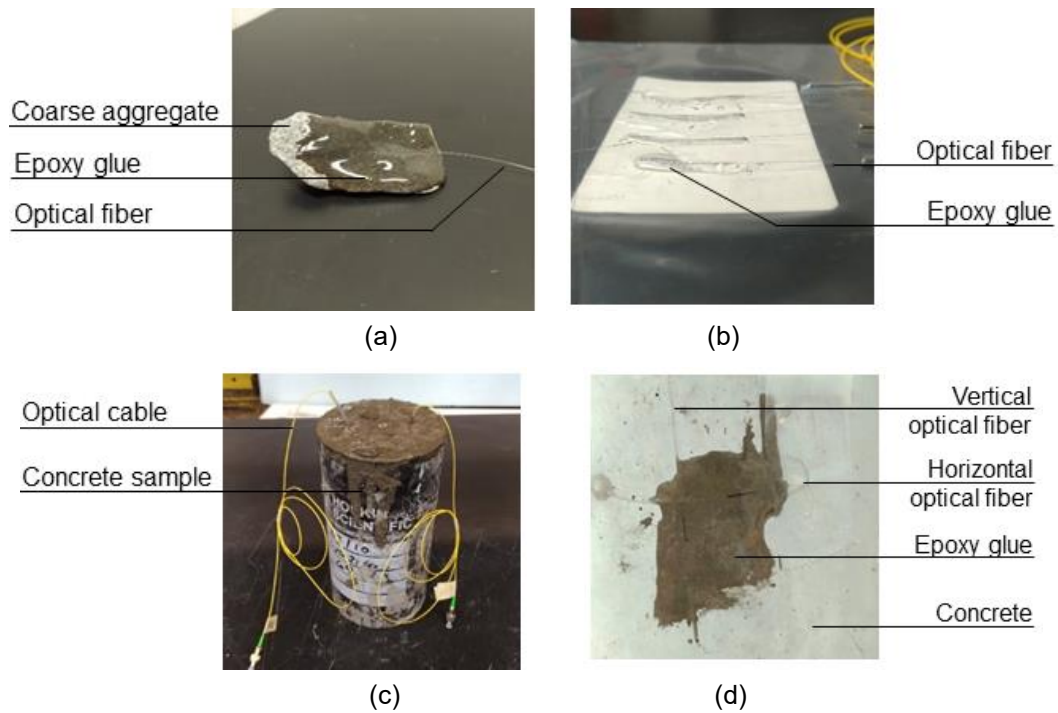


Figure 3.1: (a) FBG on aggregate, (b) FBG epoxy coating, (c) sample after casting and (d) sensor glued to the sample surface

Table 3.2: Sensors positions and directions on concrete samples

FBG positioning	Internal and external	External		
Samples	4	4	4	12

The cylinders were left to harden for 48 h before performing the initial length reading, after that they were stored at 38 °C and 100% R.H. and monitored for length changes regularly. As per ASTM C 1293, the samples were cooled to 23 °C for 16 ± 4 h prior to periodic expansion measurements. The metallic stud expansions were measured with the aid of a micrometer with a 1µm precision (equivalent to 0.0005% variations in a 200 mm sample), and the FBG at the same ages had their reflected signal monitored with the use of an optical spectrum analyzer (Yokogawa, AQ6370) with a 50pm resolution (equivalent to a 40µm/m strain resolution or 0.004% variations).

4. RESULTS AND DISCUSSION

4.1 Length change

From the length measurements performed using a micrometer, it was possible to observe the sample expansion over time, as per Figure 4.1. The error bars represent the standard error calculated from 12

samples. From the collected data, it was possible to observe a 0.03% reduction in the sample length in the first 31 days related to early age shrinkage of the concrete, followed by an expansion of around 0.11% after 39 days caused by the AAR effect on the coarse aggregate. The expansion slowly reduced until 70 days. However, this behavior was unexpected and was not observed in previous studies. Additional investigations would be required to verify if there was any factor that could have delayed the AAR reaction such as temperature variations or depletion of water in the curing system.

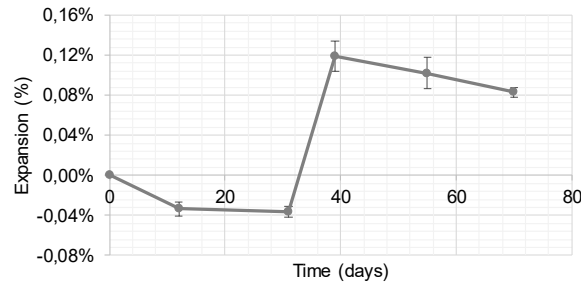


Figure 4.1: Concrete length expansion over time using a micrometer

4.2 Fiber Bragg Grating (FBG)

For the FBG sensors, it was possible to notice that the epoxy glue induced an average initial shrinkage of $-20 \mu\text{m/m}$ that was ignored after the initial readings, demonstrating thus, a considerable influence of the glue on the expansion results. Figure 4.2a shows the vertical strain obtained from the FBG sensors glued in the concrete surface. The error bars represent the standard error of the mean calculated from 12 samples. It is possible to observe a small expansion in the early days ($4 \mu\text{m/m}$), followed by a reduction in the strain, reaching an average of $-92 \mu\text{m/m}$ after 39 days.

This behavior can be confirmed by the reflected spectrum obtained during the tests (Figure 4.2b). Initially, the sensor presented a $1552,7\text{nm}$ peak, after 12 days the signal was dislocated to a higher wavelength, indicating an increase in the deformation of the optical fiber causing a change in the period of the microstructure and, consequently, in the Bragg wavelength. After that age, the peak moved to lower wavelengths, resulting in shrinkage results. Variations in the intensity of the reflected spectrum were not considered in this study since they should not influence the strain measurements.

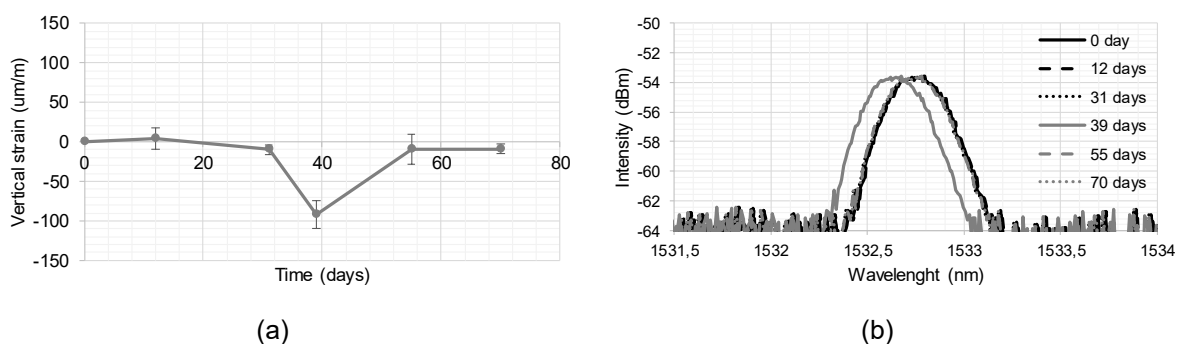


Figure 4.2: (a) External FBG vertical strain and (b) FBG reflected spectrum

Although those results display an opposite behavior when compared to the length expansions, FBG sensors are able to measure the sample strain within a 1mm length, while the metallic studs allow 200mm length measurements. Therefore, unless the cement paste on the surface of the concrete develops an expansion within the FBG region, the sensor will not be able to evaluate the overall behavior of the sample. It is worth mentioning again that only the blue colored section of the optical fiber in Figure 3.1d represents the area where the sensor performs the strain measurement.

The development of cracks through the concrete and the induced expansion around the coarse aggregates may increase the internal pressure on the paste, resulting in a negative strain on the surface of the sample. This compression of the paste between aggregates is considered before the crack

propagation and free expansion in some constitutive AAR models [6,29,39]. After the crack propagation, the internal tension should decrease, which could explain the decrease in the vertical strain observed in Figure 4.1 after 55 days to 70 days. Hence, it was possible to observe the starting day of the crack propagation due to AAR using the FBG sensor.

Regarding the FBG pairs in the vertical positions, those sensors presented a 0.1% variation on the readings, while the sensors located at different parts of the sample (aggregate, paste, and surface) presented up to 460% variation at 39 days and 4400% at 55 days, as shown in Figure 4.3.

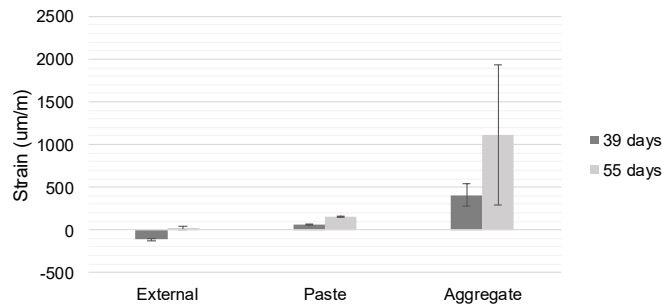


Figure 4.3: Strain in different parts of the concrete

From the results, it is possible to observe a shrinkage in the surface of the samples at early ages followed by a small positive strain, as already discussed in Figure 4.1. However, positive strains were obtained in the internal sensors, likely due to gel expansion. The paste presented a 61 $\mu\text{m/m}$ average strain at 39 days, and a 156 $\mu\text{m/m}$ at 55 days. Likewise, the aggregates presented deformations up to 1110 $\mu\text{m/m}$ strain (equivalent to 0.11%) after 55 days. Although the internal sensors presented lower expansions when compared to the total length change, they presented positive values indicating an actual expansion. Hence, the use of FBG sensors embedded in the samples or attached to aggregate particles might allow a more precise evaluation of AAR induced mechanism than at the sample's surface. It was not possible to find in the literature any works related to the evaluation of the aggregate particles swelling for comparison purposes since electronic sensors usually suffer from oxidations and are too large to be properly glued to the aggregate's surface. Finally, regarding the vertical and horizontal measurements acquired by the FBG sensors (Figure 4.4a), it was not possible to observe a correlation or similar results. Furthermore, it was not possible to obtain a proper relationship between the vertical strain and the length change results (Figure 4.4b).

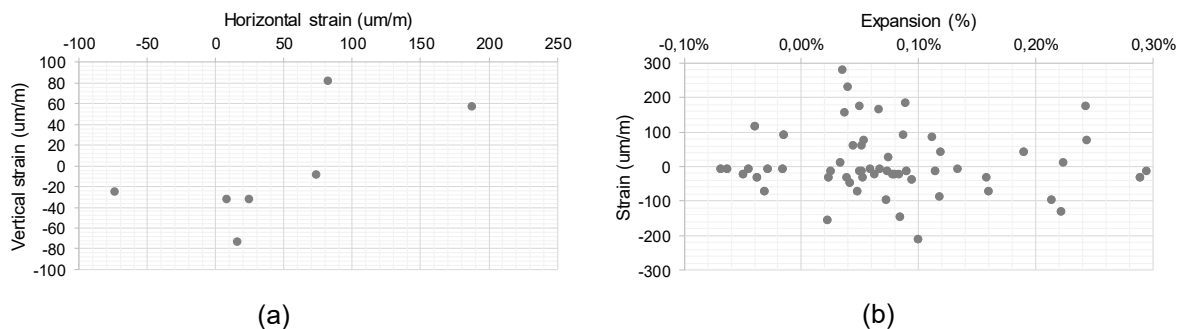


Figure 4.4: Correlations between (a) vertical and horizontal strain and (b) expansion and strain

4.3 Suggestions for future studies

Several authors were able to measure concrete deformations due to loadings by applying FBG sensors on the concrete surface [18,20,25,42,46]. However, from the results obtained in this research, it was possible to understand that the application of FBG on the surface of deteriorated and cracked concrete will not promote an accurate measurement of the expansion due to internal swelling reactions such as ASR. Therefore, to measure the overall expansion of the sample, some improvements in the

instrumentation procedures could ensure proper measurement. Figure 4.5 shows possible modifications to the FBG sensor positioning for internal and external instrumentation.

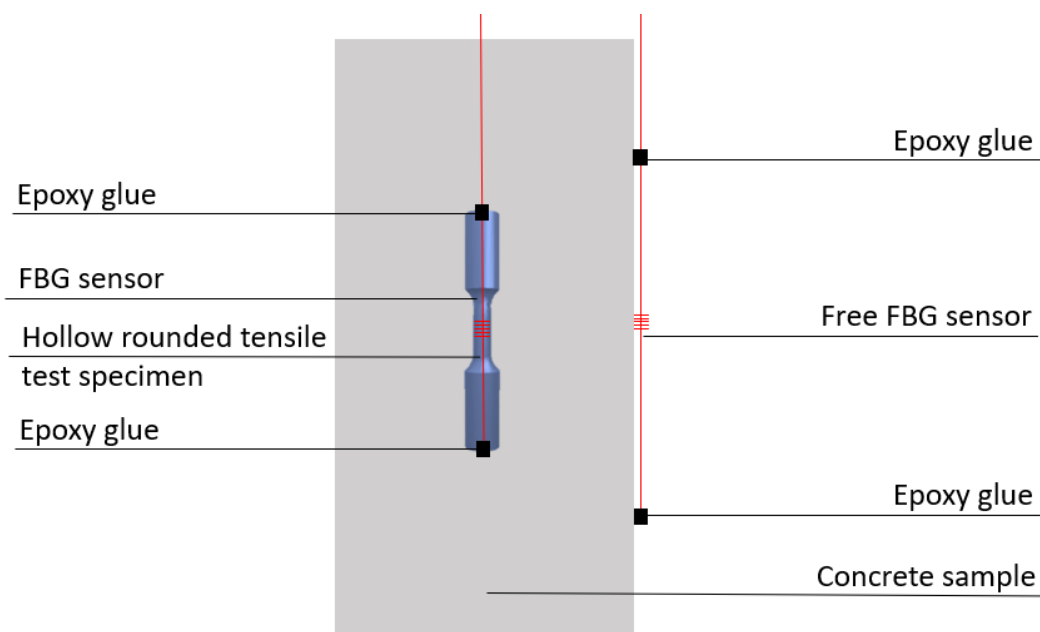


Figure 4.5: Proposed improvements for AAR expansion measurements using FBG sensors

Since the strain measurement on a specific location at the sample's surface will not represent the concrete overall expansion, for the external instrumentation it would be required to glue the optical fiber on the sample extremities, leaving the FBG length free to deform without contacting the specimen. Also, a small initial tensile should be applied to the optical fiber to allow any shrinkage measurement in the initial days. It must take into consideration that superficial shrinkage at early ages is higher than internal shrinkage, therefore, the sample instrumentation could be performed after 28 days to reduce the influence of shrinkage in the AAR expansion measurements.

For the internal measurements, the instrumentation of the aggregate showed promising results. However, for the internal paste expansion, a larger hollow metallic piece is also proposed. To ensure the sensor anchoring to the concrete, ASTM E8 metallic tensile test specimens [3] could be used. The metallic piece should be drilled, allowing the FBG positioning inside it. This way, it would be possible to also glue the optical fiber extremities, allowing a free sensor deformation inside the drilled hole. Finally, another improvement for FBG measurements would be the use of more precise equipment such as FBG interrogators with 1pm precision (50 times more precise than the optical spectrum analyzer available for this study).

5. CONCLUSION

In this work, FBG sensors were used to monitor concrete specimens affected by ASR to verify their feasibility for assessing induced expansion over time. The main conclusions of the research are presented hereafter:

- Among the several methods for ASR assessment, the use of metallic studs is still one of the most reliable ways to evaluate concrete induced expansion over time;
- Although FBG sensors present an interesting sensibility for strain measurements, its use for monitoring concrete expansion at the sample's surface did not provide a precise overall measurement, since ASR-induced expansion and crack initiation/propagation induce a local negative strain on the sample.
- It was not possible to observe any correlation between the vertical and horizontal measurements on the concrete surface. Moreover, correlations between the strain and manual expansion measurements were also not good.

- The instrumentation of the aggregate particles inside the concrete samples showed some promising results, with an 1110 $\mu\text{m/m}$ strain (equivalent to 0.11%) after 55 days. This expansion was quite close to the one observed with the use of metallic studs (i.e. 0.12%) at the same age.
- Simple modifications with the use of metallic pieces could allow better instrumentation of concrete samples during the monitoring of internal swelling reactions as proposed in this paper.

6. ACKNOWLEDGMENTS

The authors would like to thank the graduate student Haiyang Wang from the Photonics Laboratory at the University of Ottawa for the assistance on the FBG measurements, as well as the graduate students from the Civil Engineering Department at the University of Ottawa, Diego Jesus de Souza and Luan Antunes, who helped with the manufacturing of the test specimens used in this project. This project was possible thanks to a scholarship from the Brazilian Coordination of Superior Level Staff Improvement (CAPES).

7. REFERENCES

- [1] ABNT, NBR 15577-1 - Agregados - Reatividade álcali-agregado Parte 1: Guia para avaliação da reatividade potencial e medidas preventivas para uso de agregados em concreto, (2018) 21.
- [2] ASTM, C1260 - Potential Alkali Reactivity of Aggregates (Mortar-Bar Method), (2014) 5.
- [3] ASTM, E8 - Standard Test Methods for Tension Testing of Metallic Materials, (2016).
- [4] ASTM, C1293 - Standard Test Method for Determination of Length Change of Concrete Due to Alkali-Silica Reaction, (2018) 7.
- [5] S. Campopiano, A. Iadicicco, F. Messina, C. Ferone, R. Cioffi, Measurement of temperature and early age shrinkage of alkali activated metakaolin using fiber Bragg grating sensors, in: EESMS 2014 - 2014 IEEE Workshop on Environmental, Energy and Structural Monitoring Systems, Proceedings, Institute of Electrical and Electronics Engineers Inc., 2014: pp. 138–142.
- [6] B. Capra, J.P. Bournazel, Modeling of induced mechanical effects of alkali-aggregate reactions, *Cement and Concrete Research*. 28 (1998) 251–260.
- [7] P.C. Chang, A. Flatau, S.C. Liu, Review Paper: Health Monitoring of Civil Infrastructure, *Structural Health Monitoring: An International Journal*. 2 (2003) 257–267.
- [8] A.N. Chester, S. Martellucci, A.M. V. Scheggi, *Optical fiber sensors*, 1st ed., Springer, California, 1987.
- [9] CSA, A23.2-25A-14 - Test Method for Detection of Alkali-Silica Reactive Aggregate by Accelerated Expansion of Mortar Bars, (2014) 690.
- [10] C.F. Dunant, K.L. Scrivener, Effects of uniaxial stress on alkali-silica reaction induced expansion of concrete, *Cement and Concrete Research*. 42 (2012) 567–576.
- [11] M. Fajkus, J. Nedoma, P. Mec, M. Pinka, M. Novak, S. Zabka, Deformation sensor composed of fiber Bragg grating and the strain gauge for use in civil engineering, in: G. Kamerman, O. Steinvall (Eds.), *Electro-Optical Remote Sensing XII*, SPIE, Berlin, Germany, 2018: p. 34.
- [12] K. Fidanboyu, H.S. Efendioglu, Fiber optic sensors and their applications, in: 5th International Advanced Technologies Symposium, Karabuk University, Karabuk, Turkey, 2018: p. 6.
- [13] B. Glisic, D. Inaudi, *Fibre Optic Methods for Structural Health Monitoring*, John Wiley & Sons, Newport Beach, 2007.
- [14] C.A.J. Gouveia, J.M. Batista, A.S.P. Jorge, Refractometric Optical Fiber Platforms for Label Free Sensing, in: *Current Developments in Optical Fiber Technology*, 1st ed., InTech, IntechOpen, 2013: p. 30.
- [15] K.T. V. Grattan, B.T.. Meggitt, *Optical Fiber Sensor Technology*, 1st ed., Springer, New York, 2000.
- [16] P. Hewlett, M. Liska, *Lea's Chemistry of Cement and Concrete*, 5th ed., Elsevier, 2019.

- [17] M.S. Islam, N. Ghafoori, A new approach to evaluate alkali-silica reactivity using loss in concrete stiffness, *Construction and Building Materials*. 167 (2018) 578–586.
- [18] G. Kaklauskas, A. Sokolov, R. Ramanauskas, R. Jakubovskis, Reinforcement Strains in Reinforced Concrete Tensile Members Recorded by Strain Gauges and FBG Sensors: Experimental and Numerical Analysis., *Sensors*. 19 (2019).
- [19] R. Kashyap, *Fiber Bragg gratings*, 2nd ed., Academic Press, Oxford, UK, 2010.
- [20] A. Khadour, J. Waeytens, Monitoring of concrete structures with optical fiber sensors, *Eco-Efficient Repair and Rehabilitation of Concrete Infrastructures*. (2018) 97–121.
- [21] J.M. Ko, Y.Q. Ni, Technology developments in structural health monitoring of large-scale bridges, *Engineering Structures*. 27 (2005) 1715–1725.
- [22] G.W. Li, C.Y. Hong, J. Dai, L. Yu, W.H. Zhou, FBG-Based Creep Analysis of GFRP Materials Embedded in Concrete, *Mathematical Problems in Engineering*. 2013 (2013) 1–9.
- [23] H. Li, D. Li, G. Song, Recent applications of fiber optic sensors to health monitoring in civil engineering, *Engineering Structures*. 26 (2004) 1647–1657.
- [24] M. Majumder, T.K. Gangopadhyay, A.K. Chakraborty, K. Dasgupta, D.K. Bhattacharya, Fibre Bragg gratings in structural health monitoring—Present status and applications, *Sensors and Actuators A: Physical*. 147 (2008) 150–164.
- [25] P. Mec, M. Stolarik, S. Zabka, M. Novak, Application of FBG in the experimental measurements of structural elements deformation from cement composites, in: G. Kamerman, O. Steinvall (Eds.), *Electro-Optical Remote Sensing XII*, SPIE, Berlin, Germany, 2018: p. 29.
- [26] P.K. Mehta, P.J.M. Monteiro, *Concrete - Microstructure, Properties, and Materials*, 4th ed., McGraw-Hill Education, Berkeley, 2013.
- [27] F. Mitschke, *Fiber Optics: Physics and Technology*, 2nd ed., Springer, Berlin, 2016.
- [28] E.M. Moser, *Medidas múltiplas de características de barrengs de concreto compactado com rolo utilizando instrumentação por fibra ótica*, Univesidade Federal do Paraná, 2006.
- [29] S. Multon, A. Sellier, M. Cyr, Chemo-mechanical modeling for prediction of alkali silica reaction (ASR) expansion, *Cement and Concrete Research*. 39 (2009) 490–500.
- [30] A. Othonos, *Fiber Bragg gratings*, *Review of Scientific Instruments*. 68 (1998) 4309.
- [31] A. Othonos, K. Kalli, *Fiber Bragg gratings - Fundamentals and applications in telecommunications and sensing*, 1st ed., Artech House Print on Demand, Norwood, 1999.
- [32] A. Quintela, C. Jauregui, J. Echevarra, J.M. Lopez-Higuera, Embedded temperature strain fibre Bragg grating sensor system validation for concrete structures, *Journal of Optics A: Pure and Applied Optics*. 4 (2002) S387–S390.
- [33] RILEM, *Recommendations for the Prevention of Damage by Alkali-Aggregate Reactions in New Concrete Structures*, 1st ed., Springer Netherlands, Dordrecht, 2016.
- [34] L. Sanchez, B. Fournier, M. Jolin, M.A.B. Bedoya, J. Bastien, J. Duchesne, Use of Damage Rating Index to Quantify Alkali-Silica Reaction Damage in Concrete: Fine versus Coarse Aggregate, *ACI Materials Journal*. 113 (2016) 395–407.
- [35] L.F.M. Sanchez, B. Fournier, M. Jolin, J. Bastien, Evaluation of the stiffness damage test (SDT) as a tool for assessing damage in concrete due to ASR: Test loading and output responses for concretes incorporating fine or coarse reactive aggregates, *Cement and Concrete Research*. 56 (2014) 213–229.
- [36] L.F.M. Sanchez, B. Fournier, M. Jolin, J. Bastien, D. Mitchell, Practical use of the Stiffness Damage Test (SDT) for assessing damage in concrete infrastructure affected by alkali-silica reaction, *Construction and Building Materials*. 125 (2016) 1178–1188.
- [37] L.F.M. Sanchez, B. Fournier, M. Jolin, J. Bastien, D. Mitchell, L.F.M. Sanchez, B. Fournier, M. Jolin, J. Bastien, D. Mitchell, Tools for assessing damage in concrete affected by AAR coming from fine and coarse aggregates, *Revista IBRACON de Estruturas e Materiais*. 10 (2017) 84–91.

- [38] L.F.M. Sanchez, B. Fournier, M. Jolin, J. Duchesne, Reliable quantification of AAR damage through assessment of the Damage Rating Index (DRI), *Cement and Concrete Research*. 67 (2015) 74–92.
- [39] V. Saouma, L. Perotti, Constitutive model for alkali-aggregate reactions, *ACI Materials Journal*. 103 (2006) 194–202.
- [40] J.C.C. Silva, *Monitoração de vibrações de estruturas com o emprego de sensores em fibra óptica*, Universidade Tecnológica Federal do Paraná, 2005.
- [41] I. Sims, A.B. Poole, *Alkali-Aggregate Reaction in Concrete: A World Review*, 1st ed., Taylor & Francis, London, 2017.
- [42] Y. Wang, C.S. Tjin, J. Hao, T.-K. Lim, K.-B. Tan, K.M. Chan, P. Moyo, J.M.W. Brownjohn, Determination of load-strain characteristics of concrete slabs by using embedded fiber Bragg grating sensors, in: P.F. Gobin, C.M. Friend (Eds.), *Fifth European Conference on Smart Structures and Materials*, International Society for Optics and Photonics, Glasgow, United Kingdom, 2000: pp. 297–304.
- [43] H. Xu, S. Wang, X. Miao, Research of three-dimensional force sensor based on multiplexed fiber Bragg grating strain sensors, *Optical Engineering*. 56 (2017) 047103.
- [44] Z. Yazdizadeh, H. Marzouk, M.A. Hadianfard, Monitoring of concrete shrinkage and creep using Fiber Bragg Grating sensors, *Construction and Building Materials*. 137 (2017) 505–512.
- [45] S. Yin, P.B. Ruffin, F.T.S. Yu, *Fiber Optic Sensors*, 2nd ed., CRC Press, New Hampshire, 2008.
- [46] R. You, L. Ren, G. Song, A Novel Fiber Bragg Grating (FBG) Soil Strain Sensor, *Measurement*. (2019).